

# IMPEDANCE STUDY OF $K_2DyV_5O_{15}$ CERAMICS

**Parthasarathi Das**

Department of Physics, Midnapore College, Midnapore, 721101,  
India, email : [psdas00@gmail.com](mailto:psdas00@gmail.com)

## ABSTRACT

The polycrystalline sample of  $K_2DyV_5O_{15}$  (KDV), a new member of the tungsten bronze structural family, was prepared by a mixed-oxide method relatively at low temperature, (i.e.,  $500^{\circ}C$ ). X-ray diffraction studies of the compound showed the formation of single phase orthorhombic crystal structure at room temperature. SEM micrograph showed the homogeneous distribution of grains throughout the sample. Electric properties were analyzed using the complex impedance spectroscopy. The bulk impedance evaluated from the Nyquist plots was observed to decrease with the rise in temperature, showing a negative temperature coefficient of resistance. The variation of ac electrical conductivity ( $\sigma_{ac}$ ) was measured in a temperature ( $-100^{\circ}$  to  $25^{\circ}C$ ) and frequency ( $10^2$ - $10^6$  Hz) range which exhibited presence of non-Debye type of relaxation. The impedance plots exhibited multiple relaxation phenomenon.

Key words: X-ray diffraction, Solid state reaction, Impedance.

## 1. Introduction

It has been found that some ferroelectric oxides of tungsten bronze (TB) family have applications such as multilayer capacitors, actuators transducers, etc

because of their reportedly high electro-optic, nonlinear-optic, photo-refractive index, pyroelectric effect and acousto-optic properties [1-7]. The TB structure consists of a skeleton framework of distorted  $\text{BO}_6$  octahedra, sharing corners in such a way that it gives rise to three different interstitial sites (A, B, C) with a general chemical formula  $[(\text{A}_1)_2(\text{A}_2)_4\text{C}_4][(\text{B}_1)_2(\text{B}_2)_8]\text{O}_{30}$ , where A site is usually filled by di- or tri valent cations, and the B site by the pentavalent ions ( $\text{Nb}^{+5}$ ,  $\text{Ta}^{+5}$  or  $\text{V}^{+5}$ ). Generally, the smallest interstice C remains vacant, and hence a revised general formula for the TB structure can be written as  $\text{A}_6\text{B}_{10}\text{O}_{30}$  for filled tungsten bronze structure. There is a large scope to develop many new materials by substituting a wide variety of cations at different interstitial sites that can tailor the physical properties of the material significantly for applications. Detailed literature survey shows that though some interesting work has been done on some TB structured compounds [7-13], not much work have been reported on structural, dielectric and impedance properties of  $\text{K}_2\text{DyV}_5\text{O}_{15}$  (a new member of TB structural family) ceramics.

## 2. Experimental Procedure

The polycrystalline sample of  $\text{K}_2\text{DyV}_5\text{O}_{15}$  (KDV) was prepared by a mixed-oxide method at relatively low temperature ( $500^\circ\text{C}$ ) using high purity (99.9%) ingredients  $\text{K}_2\text{CO}_3$ ,  $\text{Dy}_2\text{O}_3$ ,  $\text{V}_2\text{O}_5$  (M/S Sarabhai M. Chemicals, India). The ingredients were thoroughly mixed in air atmosphere for 1h and then in methanol for another hour. The mixed powder was repeatedly fired at different temperatures ( $500$ - $550^\circ\text{C}$ ) and finally calcined at  $500^\circ\text{C}$  for 7 h in an alumina crucible. The formation of the compound was checked by X-ray diffraction (XRD) technique. The calcined powder (mixed with small amount of PVA “polyvinyl alcohol”) was cold pressed into cylindrical pellets at a pressure of  $4 \times 10^6 \text{ Nm}^{-2}$ . PVA was burnt out during the high-temperature sintering. The pellets were polished by fine emery paper to make the surfaces flat and parallel. The flat surfaces were coated with high purity conducting silver paint. After electroding, the sample was dried at a temperature of  $150^\circ\text{C}$  for 4 h to remove all moistures, and then brought to room temperature before taking any electrical measurements. Preliminary structural properties were studied by X-Ray diffractometer (Rigaku Miniflex, Japan) using  $\text{CuK}\alpha$  radiation ( $\lambda=1.5405 \text{ \AA}$ ) in a wide range of Bragg angles  $2\theta$  ( $20^\circ \leq 2\theta \leq 80^\circ$ ) with a scanning rate of  $4^\circ/\text{min}$ . The electrical properties were obtained by a computer controlled LCR meter (HIOKI Model: 3532) in a wide range of frequency ( $10^2$ - $10^6\text{Hz}$ ) at different temperatures ( $-100^\circ\text{C}$ - $20^\circ\text{C}$ ).

### 3. Experimental results and discussion

#### 3.1 Structural analysis

Fig.1 shows the XRD pattern of  $K_2DyV_5O_{15}$  (KDV) at room temperature. All the peaks of KDV were indexed in various crystal systems using computer software “POWD”

[14]. The unit cell parameters were selected on the basis of good agreement between observed (obs) and calculated (cal) interplanar spacing  $d$  ( $\sum (d_{obs}-d_{cal}) = \text{minimum}$ )

spacing. The lattice parameters refined by the method of least-squares, are found to be

$a=16.214(35) \text{ \AA}$ ,  $b=17.646(35) \text{ \AA}$ ,  $c=3.892(35) \text{ \AA}$  (the number in parenthesis is estimated standard deviation) which are in good agreement with those of reported ones [15] for the TB compounds. It was not possible to determine the space group with the limited powder data. The crystallite size (P) of LSV was roughly estimated from the broadening of few XRD peaks (in a wide  $2\theta$  range) using the Scherrer's equation,  $P=K\lambda / (\beta_{1/2}\cos\theta_{hkl})$ , (where  $K=\text{constant}=0.89$ ,  $\lambda = 1.5405 \text{ \AA}$  and  $\beta_{1/2} = \text{peak width of the reflection at half intensity}$ ). The average value of P was found to be 32 nm [15]. The effect of strain, instruments, and other defects on the broadening has been ignored for the calculation of P. Fig. 1 (inset) shows the SEM micrograph of the sample, which clearly shows uniform grain distribution over the surface with certain degree of porosity average grain size (S) 3  $\mu\text{m}$ .

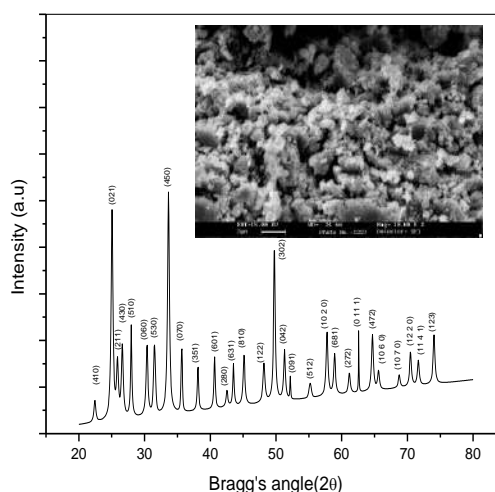


Fig.1 XRD pattern of (KDV) at room temperature

### 3.2 Dielectric Analysis:

The variation of  $\epsilon_r$  and  $\tan\delta$  of  $K_2DyV_5O_{15}$  with frequency is shown in Fig. 2. It is observed that both  $\epsilon_r$  and  $\tan\delta$  decrease with frequency which is a general feature of polar dielectric materials. The high value of  $\tan\delta$  is observed due to the lossy characteristic of the material.

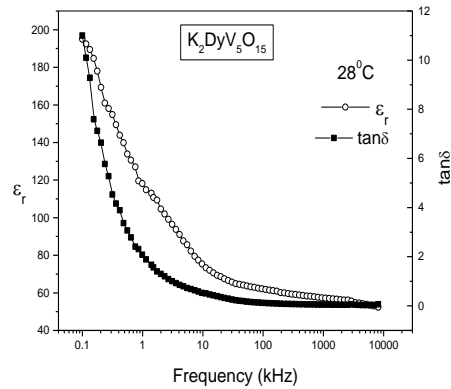


Fig.2 Variation of  $\epsilon_r$  and  $\tan\delta$  with frequency at room temperature

### 3.3 Complex Impedance Spectroscopy study

Complex impedance spectrum is a novel and effective technique to study the electrical response of dielectric or ionic materials. The frequency dependence of electrical

properties of a material is often represented in terms of complex impedance ( $Z^*$ ):  $Z^*(\omega) = Z' - jZ'' = R_s - \frac{j}{\omega C_s}$ , where ( $Z', Z''$ ) are the real and imaginary components of impedance with  $j = \sqrt{-1}$  (the imaginary factor),  $C_0 =$  vacuum capacitance.

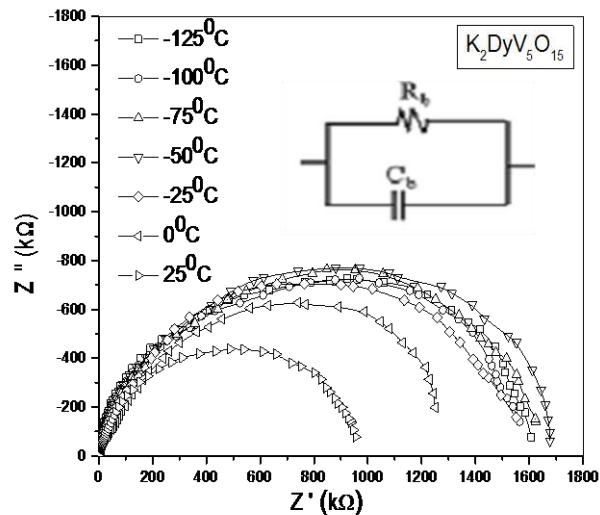


Fig.3 Variation of imaginary part with real part of complex impedance

Fig. 3 plots the imaginary part of the complex impedance ( $Z''$ ) against real part of complex impedance ( $Z'$ ) of the sample in the complex plane at different

temperatures (25<sup>0</sup>C to -125<sup>0</sup>C). The figure shows semicircular arcs. These semicircular arcs can be attributed to the bulk properties of the material and can be assigned to the parallel combination of the bulk resistance ( $R_b$ ), and bulk capacitance ( $C_b$ ). The semicircular arcs with decreasing diameter on increasing temperature, suggest that the bulk resistance of the sample (which is the intercept of the semicircular arc on the  $Z'$  axis) decreases with temperature. This implies that the sample exhibits negative temperature coefficient of resistance, which is a fundamental characteristic of a semiconductor. The second semicircular arcs

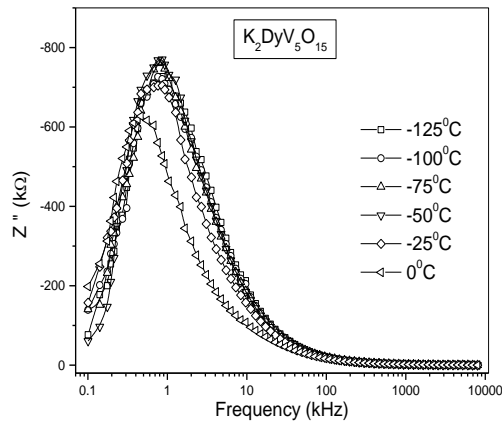


Fig.4 Variation of  $Z''$  with frequency at different temperatures

The variation of  $Z''$  with frequency (Fig. 4) shows the presence of asymmetric peaks at the different temperatures. The shift in the peak frequency towards the higher side of the frequency range arises possibly due to the presence of space charge at higher temperatures. The asymmetric broadening of the peaks suggests that multiple

which generally appears in the low frequency domain and at high temperatures indicating the evidence of grain boundary effects in the material is not observed in our range of measurement. The grain and grain boundary effects can be modeled as cascading of parallel RC combination in accordance with brick layer model, as represented in terms of the equivalent circuit at inset.

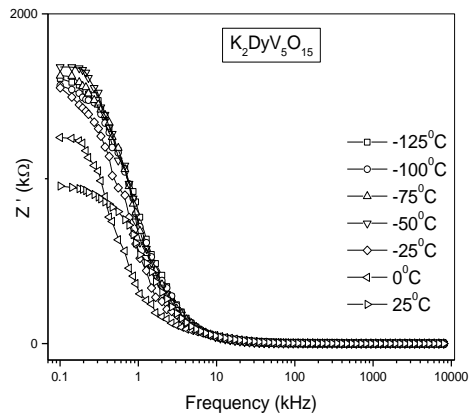


Fig.5 Variation of  $Z'$  with frequency at different temperatures

relaxation phenomenon is present in the material, with their own discrete relaxation time depending on the temperature. The spread of the relaxation time, as indicated by the peak broadening, may be interpreted as comprising of two equilibrium processes related to the immobile species at lower temperature and defects at higher temperatures.

Fig. 5 shows that  $Z'$  decreases with the rise of temperature and frequency. This indicates that ac conductivity rises with increasing temperature and frequency. The values of  $Z'$  is found to merge above certain frequency. This may be attributed to the lowering of barrier properties of the sample with temperatures and then space charge would be emitted, which would enhance the conductivity and reduce the impedance properties.

### 3.4 Electrical conductivity analysis

The electrical conductivity of the material has been investigated at different temperatures over a wide range of frequencies. Frequency independent conductivity  $\sigma_{dc}$  and the ac conductivity  $\sigma_{ac}$  has also been evaluated from complex impedance spectrum and observed as a function of temperature.

The typical variation of  $\sigma_{dc}$  as a function of temperature has the characteristics that the conductivity increases with the increment of temperature. This is a typical Arrhenius type behavior:  $\sigma_{dc} = \sigma_0 \exp(-E_a/k_B T)$ , where  $\sigma_0$  is the pre exponential factor  $E_a$  is the activation energy and  $k_B$  is the Boltzmann constant. The activation energy can be calculated from the slope of straight line. A slight departure from the linear dependence of conductivity on the temperature has been noticed at low temperature. This can be attributed to the Mott's type hopping phenomenon. The activation energy calculated from the slope of the graph is The smaller value of activation energy ( $E_a$ ) in the low temperature region may be due to the electron hopping between the ions of different vacancies At low temperature with low

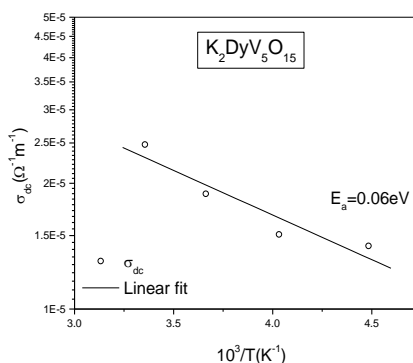


Fig. 6 Variation of dc conductivity with temperature

activation energy thermal energy is just sufficient to allow the migration of atoms and ions into the vacancies already associated in the compound. The conductivity increases with temperature. This supports the NTCR behaviour of the material.

The variation of ac conductivity as a function of frequency (conductivity spectrum) at different temperatures is shown. The conductivity pattern can be

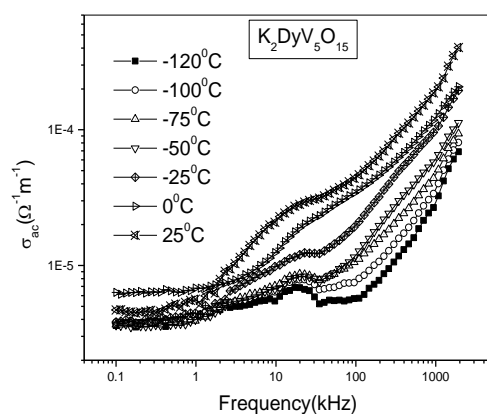


Fig.7 Variation of ac conductivity with frequency at different temperatures

divided into two parts. First at low temperatures a continuous dispersion curve of conductivity is observed. In the lower frequency region the magnitude of conductivity has appreciably distinct values whereas the conductivity pattern approaches close to each other in the high frequency region for the same temperature region. This may be attributed to the space charge dependent

region.

When ac conductivity is observed as a function of temperature at different frequencies then we observe that  $\sigma_{ac}$  rises with temperature having higher value at higher frequencies. A higher magnitude of  $\sigma_{ac}$  for the sample at higher frequencies in lower temperature is expected in view of strong frequency dependence under these conditions. As temperature increases the conductivity of the material at different frequencies approach each other. This may be due to the release of space charge. This indicates that electrical conduction is a thermally activated process.

#### 4. Conclusions

The polycrystalline sample of  $K_2DyV_5O_{15}$  (KDV), a new member of TB structural family, was prepared by a mixed oxide method at relatively low temperature ( $500^{\circ}C$ ). Preliminary X-ray analysis exhibited the orthorhombic crystal structure of the compound at room temperature. Impedance spectroscopy was used to characterize the electric properties of the material. The material showed the NTCR behaviour which is the characteristics of a semiconductor.

Study of the temperature dependence of ac conductivity showed that the ac conductivity of the material follows the Arrhenius equation; and the conduction mechanism of the material might be due to the hopping of the charge carriers.

### References:

1. X. M. Chen, Y. H. Sun, X. H. Zheng, J. Eur. Ceram. Soc. **23**, 1571 (2003).
2. L. Fang, L. Chen, H. Zheng, C. L. Diao, R. Z. Yuan, Mater. Lett. **58**, 2654 (2001).
3. X.M. Chen, Y.Yuan, Y.H. Sun, J. Appl. Phys. **97**, 074108 (2005).
4. K. Uchino, Ceram. Inter. **21**, 309 (1995).
5. R.R. Neurgaonkar, J.R. Oliver, J.G. Nelson, Mater. Res. Bull. **26**, 771 (1991).
6. E.L. Venturini, E.G. Spencer, A.A. Ballman, J. Appl. Phys. **40**, 1622 (1969).
7. S. Sakamoto, T. Yazaki, Appl. Phys. Lett. **22**, 429 (1973).
8. E.A. Geiss, B.A. Scott, G.Burns, D.F.O’Kane, A. Segmuller, J. Amer. Ceram. Soc. **52**, 276 (1969).
9. G. Burns, F. H. Dacol, Phy. Rev. B **40**, 4012 (1984)
10. J. Ravez, H.El Alaoui- Belghiti, M. Elaatmani, A. Simon, Mater. Lett. **47**,159 (2001)
11. B. Behera, P. Nayak, R.N.P.Choudhary, Mater.Lett. **61**, 3859(2007)
12. B. Behera, P. Nayak, R.N.P.Choudhary, Phys. Status Solidi A, **204**, 2479 (2007)
13. P.R. Das, R. N. P. Choudhary, B. K. Samantray, Mater.Chem.Phys, **101**, 228 (2007)
14. E.Wu, POWD, An Interactive Powder Diffraction Data Interpretation and Indexing Program, Ver. 2.1, School of Physical Sciences, Flinders University South Bedford Park, SA 5042 Australia.
15. B. Behera, P. Nayak, R.N.P.Choudhary, Mater. Lett. **61**, 3859(2007)